Gyrotropy of a Metamolecule: Wire on a Torus

N. Papasimakis,* V. A. Fedotov, K. Marinov,† and N. I. Zheludev

Optoelectronics Research Centre, University of Southampton, SO17 1BJ, United Kingdom

(Received 11 June 2009; revised manuscript received 29 July 2009; published 26 August 2009)

Sharing topology with numerous organic molecules, a wire helix bend into a torus gives a curious object with a gyrotropic behavior which is far from obvious. While a continuous constant current in opposite sections of the torus would create mutually cancelling contributions to its gyrotropic response, an array of tori can show strong circular dichroism linked to the excitation of standing current waves. Here we present the experimental study of optical activity in a chiral toroidal metamaterial and discuss its response in terms of multipole moments, including the elusive toroidal moment.

DOI: 10.1103/PhysRevLett.103.093901 PACS numbers: 41.20.Jb, 78.20.Ek

Toroidal, doughnut-shaped structures are ubiquitous in nature, appearing on scales which range from the subatomic [1,2] to the astronomical [3]. On the molecular level, the torus shape is preferred by numerous biological and chemical macromolecules, such as DNA condensates [4], proteins [5,6], bacteriophages [7], and oligosaccharides [8] (see Fig. 1). Toroidal symmetries are also encountered frequently in solid-state systems including fullerenes [9,10] and ferroelectrics [11,12]. However, the interactions of toroidal structures with electromagnetic radiation are not well understood. Within the framework of classical electrodynamics it has been shown that toroidal currents could be nonradiating [13,14] while interactions between toroidal currents could allegedly violate Lorentz reciprocity [15], thus in principle allowing for asymmetric energy and information transfer between biological molecules. Nevertheless, experimental investigations of the electromagnetic response of such structures are rare [16–18]. In this Letter, we investigate the gyrotropic properties of toroidal media by studying a new chiral metamaterial consisting of toroidal wire windings.

In contrast to ''helical'' gyrotropic media, where handedness is usually associated with the direction of a ''twist vector'' following the corkscrew law along a helicity axis, the situation is more complicated when the structure possesses toroidal symmetry [see Fig. 1(c)]. Here the twist vector rotates along the torus. However, although no helicity axis exists, the structure has two well-defined enantiomeric forms, corresponding to different directions of the winding. We show that the complex geometrical chirality of toroidal windings can lead to strong resonant optical activity that is linked to the excitation of multinodal standing-wave current configurations on the toroid.

Based on the structure of Fig. 1(c), we manufactured and characterized a microwave metamaterial consisting of an array of toroidal wire windings (see Fig. 2), etched from a 35 μm-thick copper cladding on both faces of dielectric bars with permittivity $\epsilon = 4.5 - 0.081i$ and thickness of 3.2 mm. The 0.3 mm-wide wire strips were connected by metal wires linking strips on opposite sides of the slab in order to create a closed toroidal wiring consisting of four full 3.2×3.5 mm rectangular loops. Polarization-sensitive transmission experiments were performed at normal incidence in an anechoic chamber using linearly polarized lens-corrected horn antennas and a vector network analyzer.

Normal incidence [along the y axis of Fig. 2(c)] measurements revealed very strong resonant circular dichroism and optical activity in the toroidal metamaterial. This is illustrated in Figs. 3(a) and 3(b), which show the circular differential (left-right) transmission $\Delta t = t_+ - t_-$ and the differential phase delay $\Delta\varphi = \varphi_+ - \varphi_-$, respectively, quantifying the circular dichroism and the polarization plane rotation, respectively. Three resonant bands of strong circular dichroism can be distinguished at around $\nu_2 = 4.5$ GHz, $\nu_4 = 7.5$ GHz, and $\nu_6 = 10$ GHz [Fig. 3(a)]. Corresponding resonant features are also seen in the cir-

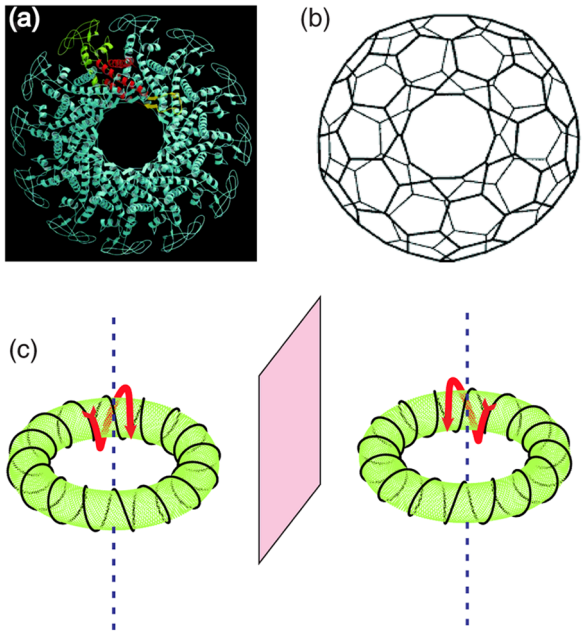

FIG. 1 (color online). Examples of chiral toroidal structures: (a) the head-tail connector of the bacteriophage ϕ29 [7]; (b) a torus-shaped fullerene [10]. (c) The enantiomeric forms of a chiral toroidal coil are connected by a mirror reflection.

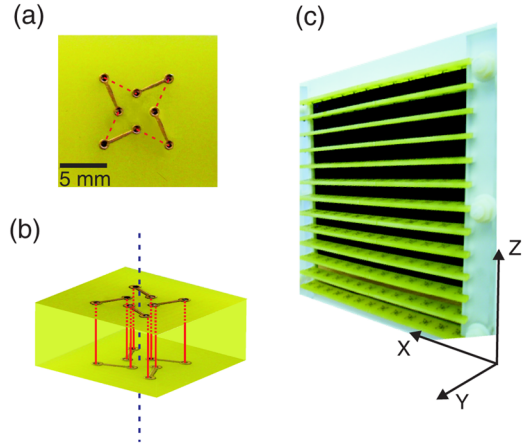

FIG. 2 (color online). (a) Top and (b) side views of the unit cell of the toroidal metamaterial. In the experimental measurements, the toroids are arranged into a 13×13 metamaterial array (c) so that the normally incident electromagnetic wave propagates perpendicular to the axes of the toroids.

cular differential phase dispersion [Fig. 3(b)]. At $\nu_4 = 7.5$ GHz, both polarization states are rejected, one more strongly than the other, while at the low- and high-frequency resonances, the polarization selective behavior is particularly strong with transmission of the nonrejected polarization remaining above 50%. At the same time, the phase derivative for orthogonal polarizations has opposite signs (not shown here), one corresponding to a forward propagating wave and the other to a backward wave, which is considered to be a manifestation of negative refraction in chiral media [19,20].

The nature of these resonances can be elucidated by numerical calculations of field and current distributions induced by the electromagnetic wave in the toroidal wire coils (Fig. 4). They clearly illustrate the origin of circular dichroism of the metamaterial. Figures 4(a) and 4(b) show the energy density maps and power flow lines (tangent to the Poynting vector at each point) near the toroidal coil under resonance conditions (at the 4 GHz dichroism band) calculated with a commercial finite element analysis software package (COMSOL 3.3). While right circular polarization interacts strongly with the left-handed coil and is strongly absorbed as indicated by the "winding" of the power flow lines in the vicinity of the wires [see Fig. 4(a)], the orthogonal polarization state propagates almost unaffected [Fig. 4(b)]. Figures 4(c) and 4(d) show the amplitude of current oscillations along the toroidal wire winding induced by the incident wave at two most prominent resonances ($\nu_2 \simeq 4$ GHz and $\nu_6 \simeq 10$ GHz). From here one can clearly see that the observed resonances are linked to the excitation of multinodal standing current waves, the form of which is disturbed by the sharp corners of the wire winding that introduce higher harmonics, as well as by the finite width of the wires and by interactions between opposite-facing loops. The spatial variation of the current configuration along the wire winding is determined by the relation between the excitation wavelength and the total wire length. Under a coarse approximation, resonances occur when the total wire length in the metamaterial unit cell is equal to an integer multiple of the excitation wavelength with an even number of nodes. Here the presence of the dielectric also has to be taken into account in the estimation of the effective wavelength. Correspondingly, the subscript numbering resonances $\nu_2 = 4.5$ GHz, $\nu_4 = 7.5$ GHz, and $\nu_6 = 10$ GHz is simply the number of nodes

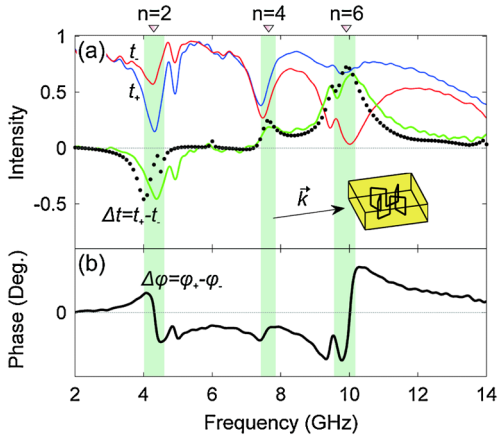

FIG. 3 (color online). (a) Transmission t for a right (blue line) and a left (red line) circularly polarized wave. The circular dichroism Δt is represented by the solid green curve (experimental) and the black solid circles (numerical). The positions of the main dichroism resonances at ν_2, ν_4, and ν_6 are marked by the green strips. Inset: Sketch of the toroidal metamaterial unit cell and direction of wave propagation. Panel (b) shows the left-right differential phase delay $\Delta\varphi = \varphi_+ - \varphi_-$.

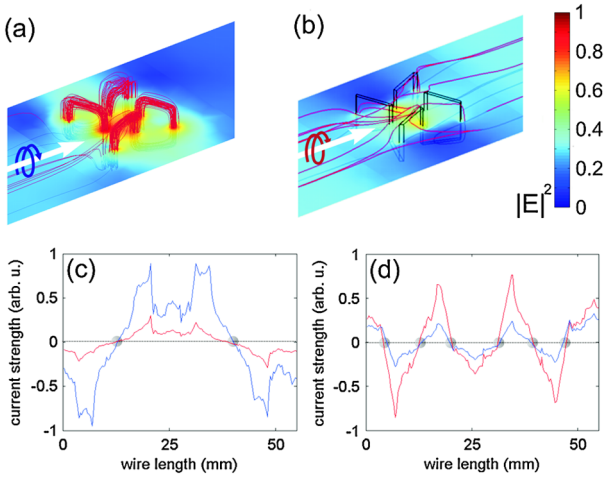

FIG. 4 (color online). Finite element simulations of toroidal metamaterial. (a) and (b) show electric density (color maps) and power flow lines at the 4 GHz resonance for a right and left circularly polarized incident wave, respectively. (c) and (d) present the induced current oscillation as a function of position on the wire winding for right (red line) and left (blue line) circularly polarized light, at the 4 and 10 GHz resonances, respectively.

in the standing current distribution. The array of tori shows strong resonant circular dichroism and circular birefringence at frequency regions where electromagnetic excitation induces a multinodal standing current wave on the wire coil with the opposite sections of the torus working in unison (ν_2 and ν_6). This means that at any given time the currents in the opposite sections of the coil flow in *opposite* directions (see sketches of idealized resonant toroidal current distributions in Fig. 5). This can be possible only in the high-frequency regime where the toroidal coil wire is much longer than the wavelength. On the contrary, in the low-frequency limit the induced currents will be in phase all along the wire, and thus the opposite sections of the torus would create mutually cancelling contributions to its gyrotropic response. An excellent agreement between the experimental and numerical results gives a good confidence in our interpretation (see Fig. 3).

The way through which gyrotropy arises in such a structure becomes even clearer within the framework of multipole theory. In general, circular dichroism arises from the coupling of parallel electric and magnetic dipole moments but can also include a contribution from the electric quadrupole moment [21–23]. In Fig. 5, the strength of the first few multipole moments is presented in terms of radiated power [24] under excitation with a linearly polarized plane wave, calculated from the induced currents [24,25]:

$$\text{electric dipole: } p_i = \frac{1}{i\omega}\int J_i dV,$$

$$\text{magnetic dipole: } m_i = \frac{1}{2}\int (\vec{r}\times\vec{J})_i dV,$$

$$\text{electric quadrupole: } Q_{ij} = \frac{1}{i\omega}\int (r_i J_j + J_i r_j) dV,$$

where $i, j = x, y, z$ and J is the current density. The strength of different multipole moments can then be compared in terms of the radiated power [24]. As expected from the relatively large size of the structure compared to the wavelength, the electric dipole moment dominates the response of the system at all frequencies, while all multipole moments resonate together at the $\nu_2 = 4.5$ GHz and $\nu_6 = 10$ GHz circular dichroism bands. More concisely, at the low-frequency resonance, the magnetic dipole is much stronger than the electric quadrupole, indicating that the main contribution to chirality comes from the electric dipole-magnetic dipole coupling. A similar situation arises at the high-frequency dichroism band ($\nu_6 = 10$ GHz). However, near the weaker $\nu_4 = 7.5$ GHz resonance, the electric quadrupole presents a pronounced resonance, while the magnetic dipole moment is weaker. The resonant character of the weak dichroism at this resonance indicates electric dipole-electric quadrupole in addition to the electric dipole-magnetic dipole coupling. This behavior arises directly from the symmetry of the structure and the supported currents as illustrated in the inset of Fig. 5 for an idealized toroid which is much smaller than the wavelength. In the ideal case, the mode with $n = 2$ nodes leads

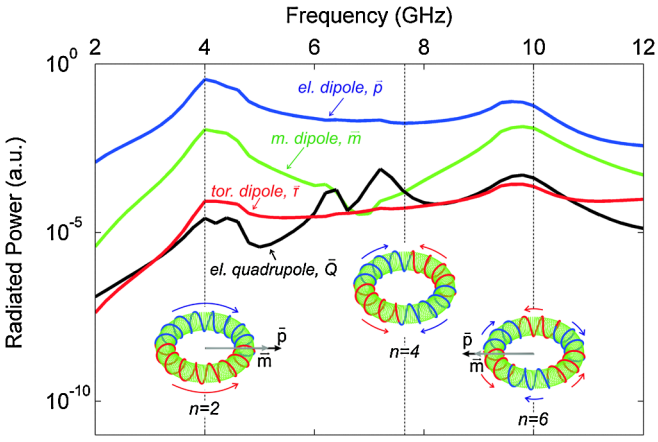

FIG. 5 (color online). Radiated power from the different multipole moments of the (numerically simulated) current configuration on the wire windings, normalized to the incident power. Insets: Idealized resonant currents modes on the toroidal solenoid and leading terms of the multipole expansion for current configurations with two, four, and six nodes (from left to right). For $n = 2$ the leading terms are the electric p and magnetic m dipole moments, while for $n = 4$, these moments vanish and the electric quadrupole moment Q dominates the response of the structure. In the case $n = 6$, both dipole and quadrupole moments are present. Dashed vertical lines show positions of gyrotropy resonances.

to strong electric and magnetic dipole moments, which have the same direction, while $n = 4$ corresponds to a dominant quadrupole excitation of the structure, where electric and magnetic dipole moments vanish. In a small ideal toroidal current, this mode is uncoupled to free space and does not interact with external radiation. In practice, however, it is excited due to the finite size of the structure, which also leads to a strong dipole component. On the other hand, the mode with $n = 6$ results in both strong dipole and quadrupole moments and thus in a more complex response.

In addition to insights in the interplay between chiral and toroidal symmetries, our experiments also provide a unique opportunity to investigate the role of the so-called toroidal moments in such electromagnetic interactions. Introduced by Zel'dovich in 1958 [1], toroidal moments are intensively discussed in the literature with only a few experiments claiming to having detected them [17,18]. It has been suggested that the complete multipole expansion requires the inclusion of toroidal moments along with the electric and magnetic ones [26]. While usually these moments can be neglected, this is not true for structures comparable to the wavelength or structures of toroidal symmetry [26], as the one considered here. Moreover, the toroidal moment is known to result in magnetoelectric coupling [27], since it enters the multipole expansion in exactly the same way as the electric moments [26]. Therefore one might expect that coupling between toroidal and magnetic moments would lead to optical activity, and the question of a toroidal contribution to the observed

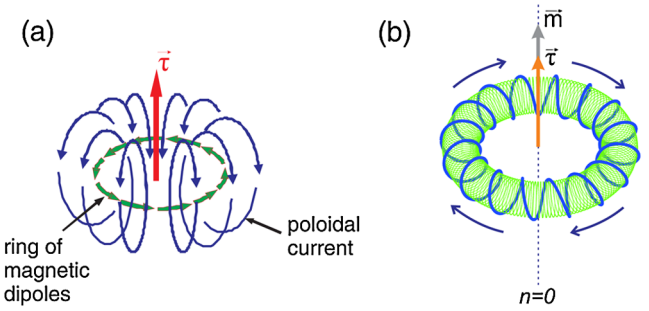

FIG. 6 (color online). Magnetic toroidal moment. A static poloidal current on a torus creates a ringlike configuration of magnetic dipoles, which in turn leads to a magnetic toroidal dipole moment τ (a). A constant current flowing along the chiral toroidal coil results in a (magnetic) toroidal τ and magnetic dipole m moments. The latter depends on the chirality of the coil (b).

chirality arises. Indeed, the studied structure is topologically suitable for supporting magnetic toroidal moments arising from a ringlike configuration of magnetic dipole moments as shown in Fig. 6(a), which in turn can be created by a poloidal current. Such a current distribution is supported by a chiral toroidal solenoid in a quasistatic regime: It corresponds to the fundamental current mode with $n = 0$, for which all electric multipole moments vanish, while strong magnetic dipole m and magnetic toroidal τ moments are supported [Fig. 6(b)]. Here the sign of the magnetic dipole depends on the chirality of the toroid and results from the component of the current directed perpendicular to the plane of the winding's loops; on the contrary, the direction of the toroidal dipole moment is independent of the chirality of the toroid [15,28]. In order to quantify the toroidal response of the metamaterial, we calculate its induced oscillating toroidal moment by the formula $\vec{\tau} = \frac{1}{10}\int[(\vec{r}\cdot\vec{j})\vec{r} - 2\vec{r}^2\vec{j}]d^3r$ and present in Fig. 5 the corresponding radiated power $P_T = \frac{\omega^6\mu_0}{12\pi c^5}|\vec{T}|^2$ [24]. At most frequencies the toroidal moment is comparable with the electric quadrupole moment, which suggests that the toroidal contribution to the metamaterial response is in general non-negligible. However, as can be seen from the radiated powers, its contribution in the gyrotropy is at best secondary, since the electric and magnetic dipole/electric quadrupole moments are much stronger at the dichroism resonances. Nevertheless, we expect that a much more pronounced toroidal response can be achieved by approaching a quasistatic regime, where a constant current flows along the toroidal wire winding [28]. Because of the symmetry of the structure, such a current configuration has a much weaker electric dipole moment which could lead to a clear manifestation of polarization effects depending on the magnetic toroidal moment.

In summary, torus-shaped molecular structures are widespread in nature; however, specifics of their electromagnetic interactions are not comprehensively understood. We investigated experimentally and numerically polarization-sensitive electromagnetic interactions in artificial toroidal media and reported strong resonant optical activity linked to the excitation of current standing waves in the toroidal coils. A multipole expansion of these current configurations revealed a nonvanishing induced oscillating magnetic toroidal moment.

The authors acknowledge the financial support of the Engineering and Physical Sciences Research Council, United Kingdom, and numerous fruitful discussions with A. D. Boardman.

*N.Papasimakis@soton.ac.uk
†Present address: STFC Daresbury Laboratory, ASTeC, Daresbury, Warrington, WA44AD, U.K.
kiril.marinov@stfc.ac.uk

[1] Y. B. Zel'dovich, Sov. Phys. JETP **6**, 1184 (1958).
[2] V. M. Dubovik and A. A. Cheshkov, Sov. J. Part. Nucl. **5**, 318 (1975).
[3] J. S. Mainstone, Nature (London) **215**, 1048 (1967).
[4] N. V. Hud and I. D. Vilfan, Annu. Rev. Biophys. Biomol. Struct. **34**, 295 (2005).
[5] M. M. Hingorani and M. O'Donnell, Nat. Rev. Mol. Cell Biol. **1**, 22 (2000).
[6] R. Kovall and B. W. Matthews, Science **277**, 1824 (1997).
[7] A. A. Simpson *et al.*, Nature (London) **408**, 745 (2000).
[8] W. Saenger *et al.*, Chem. Rev. **98**, 1787 (1998).
[9] J. Liu *et al.*, Nature (London) **385**, 780 (1997).
[10] A. Ceulemans, L. F. Chibotaru, and P. W. Fowler, Phys. Rev. Lett. **80**, 1861 (1998).
[11] A. A. Gorbatsevich and Y. V. Kopaev, Ferroelectrics **161**, 321 (1994).
[12] I. I. Naumov, L. Bellaiche, and H. X. Fu, Nature (London) **432**, 737 (2004).
[13] G. N. Afanasiev and V. M. Dubovik, Phys. Part. Nucl. **29**, 366 (1998).
[14] A. D. Boardman, K. Marinov, N. I. Zheludev, and V. A. Fedotov, Phys. Rev. E **72**, 036603 (2005).
[15] G. N. Afanasiev, J. Phys. D **34**, 539 (2001).
[16] N. A. Tolstoy and A. A. Spartakov, JETP Lett. **52**, 161 (1991).
[17] K. Sawada and N. Nagaosa, Phys. Rev. Lett. **95**, 237402 (2005).
[18] V. A. Fedotov *et al.*, New J. Phys. **9**, 95 (2007).
[19] J. B. Pendry, Science **306**, 1353 (2004).
[20] V. M. Agranovich, Y. N. Gartstein, and A. A. Zakhidov, Phys. Rev. B **73**, 045114 (2006).
[21] A. D. Buckingham and M. B. Dunn, J. Chem. Soc. A **1971**, 1988 (1971).
[22] I. P. Theron and J. H. Cloete, IEEE Trans. Microwave Theory Tech. **44**, 1451 (1996).
[23] Y. P. Svirko and N. I. Zheludev, *Polarization of Light in Nonlinear Optics* (Wiley, New York, 2000).
[24] C. Vrejoiu, J. Phys. A **35**, 9911 (2002).
[25] R. E. Raab and O. L. de Lange, *Multipole Theory in Electromagnetism* (Oxford University, New York, 2005).
[26] V. M. Dubovik and V. V. Tugushev, Phys. Rep. **187**, 145 (1990).
[27] M. Fiebig, J. Phys. D **38**, R123 (2005).
[28] K. Marinov *et al.*, New J. Phys. **9**, 324 (2007).